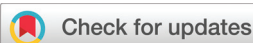


## RESEARCH ARTICLE

View Article Online  
View Journal | View IssueCite this: *Org. Chem. Front.*, 2024, **11**, 3639Received 29th February 2024,  
Accepted 9th May 2024

DOI: 10.1039/d4qo00390j

rsc.li/frontiers-organic

# Light-mediated catalytic enantioselective difluoroalkylation of $\beta$ -ketoesters via phase-transfer catalysis†

Callum E. Adams and Craig P. Johnston \*

We report a phase-transfer-catalysed asymmetric  $\alpha$ -difluoroalkylation of  $\beta$ -ketoesters through visible light-promoted radical generation. This methodology affords quaternary stereocentres with mild enantioenrichment and isolated yields up to 99%. Through mechanistic investigations, we have determined that the reaction proceeds via difluoroalkyl radical generation arising from an *in situ* electron donor–acceptor complex capable of absorbing visible light. Extensive optimisation of the reaction parameters was carried in an attempt to overcome a facile racemic background reaction.

## 1. Introduction

Owing to their growing role in materials science, agrochemicals, and pharmaceuticals the introduction of difluoroalkyl groups has become an area of particular interest.<sup>1–3</sup> This is due to the well-established improvements in metabolic stability, lipophilicity, and bioavailability gained by incorporating fluorine-containing functional groups into organic molecules.<sup>4–6</sup> To install difluoroalkyl moieties enantioselectively typically requires the use of transition metals either as photocatalysts or to provide a chiral environment with an enantiopure ligand.<sup>7–13</sup> In the context of difluoroalkyl radicals, their enantioselective incorporation into a molecule has been limited to two examples, but both require the use of transition metals. First, Lu and Xiao harnessed a chiral nickel Lewis acid catalyst with an iridium photocatalyst for the asymmetric difluoroalkylation of  $\beta$ -ketoesters (Fig. 1A).<sup>12</sup> Later, Xu synthesised enantioenriched *gem*-difluoroalkyl containing  $\gamma$ -keto amides using a chiral-at-rhodium(III) complex and an Ir photocatalyst (Fig. 1B).<sup>10</sup> Therefore, due to the lack of enantioselective protocols for introducing difluoroalkyl groups and the current constraint of using unsustainable, toxic, and expensive transition metal catalysts we sought to explore an alternative strategy. Primarily we were intrigued by light-initiated methods that remove the need for exogenous photocatalysts. For example, a system developed by Melchiorre and co-workers realised the  $\alpha$ -trifluoromethylation and perfluoroalkylation of  $\beta$ -ketoesters in the absence of transition metals

(Fig. 1C).<sup>14</sup> This transformation was rendered asymmetric through the use of an organocatalytic phase-transfer catalyst (PTC).<sup>15–21</sup> Aside from providing a chiral environment the PTC also facilitates the formation of an electron donor–acceptor (EDA) complex by solubilising the enolate of the  $\beta$ -ketoester in a non-polar solvent so that it can interact with the electron-deficient perfluoroalkyl iodide. Formation of EDA species can manifest pronounced characteristics and they can be identified

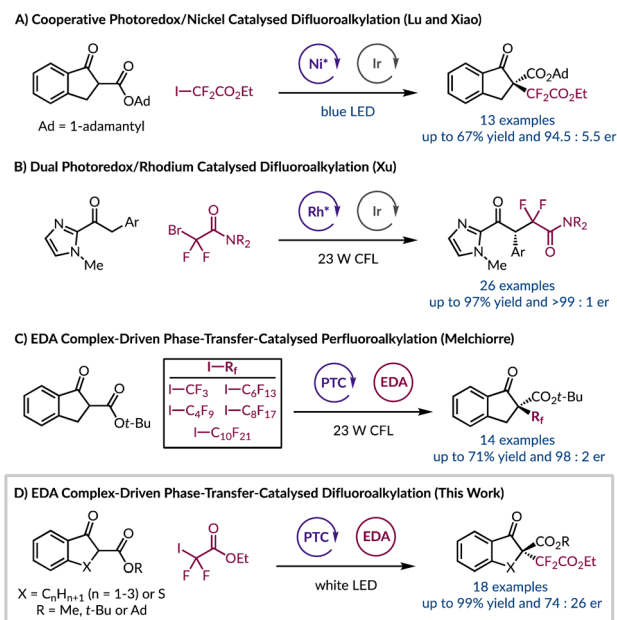


**Fig. 1** (A and B) Previous asymmetric difluoroalkylation reactions; (C) enantioselective perfluoroalkylation using a chiral phase-transfer catalyst; (D) organocatalytic enantioselective difluoroalkylation of  $\beta$ -ketoesters.

EaStCHEM, School of Chemistry, University of St Andrews, St Andrews, Fife, KY16 9ST, UK. E-mail: cpj3@st-andrews.ac.uk

† Electronic supplementary information (ESI) available. See DOI: <https://doi.org/10.1039/d4qo00390j>



through a number of different methods.<sup>22–28</sup> Importantly, an EDA complex is capable of absorbing visible light, and undergoing a subsequent single electron transfer process, to afford a desirable radical intermediate derived from the electron acceptor. We sought to build on this observation by exploring a range of ketones and  $\beta$ -ketoesters to stereoselectively incorporate the difluoroalkyl moiety under sustainable, metal-free conditions. Herein, we report our endeavour to harness organocatalytic phase-transfer conditions with the generation of tertiary radicals resulting from an EDA complex, to afford enantioenriched  $\alpha$ -difluoroalkylation of  $\beta$ -ketoesters (Fig. 1D).

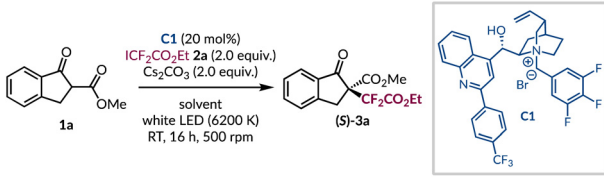
## 2. Results and discussion

### Initial reactivity and optimisation

For the initial investigations,  $\beta$ -ketoester **1a** was selected as the model substrate for difluoroalkylation under asymmetric phase-transfer-catalysed conditions, as it has been shown to be applicable to both EDA complex formation and phase-transfer catalysis.<sup>14–16</sup> Likewise, ester **2a** is commercially available and when subjected to a variety of photochemical conditions is known to give the required difluoroalkyl radical.<sup>29–37</sup> An initial result gave the desired product **3a** in 10% yield under previously optimised reaction conditions (Table 1, entry 1),<sup>14</sup>

albeit with very poor asymmetric induction. Using this catalytic system an extensive solvent screen was undertaken (see ESI page S15†), and four solvents ( $\text{CH}_2\text{Cl}_2$ ,  $\text{CHCl}_3$ , *t*-BuOAc, and *t*-BuPh) showed a marginal improvement in enantioselectivity, as well as improved yields of product **3a** (Table 1, entries 2–5). Initially, we thought the removal of catalyst **C1** would impede the transformation, but we were surprised to find that a significant racemic background reaction occurs in both *t*-BuOAc and *t*-BuPh (Table 1, entries 6 and 7). At this stage, we hypothesised that the cesium cation was sufficiently solubilising to promote enolate formation and due to the less prominent background reactivity observed in *t*-BuOAc, optimisation continued using it as the solvent. Subsequently, a base screen was carried out in an attempt to minimise the uncatalysed pathway (see ESI page S16†). In general, alternative bases only resulted in lower yields of product **3a** with reduced levels of enantioenrichment (Table 1, entries 8 and 9). During this phase of the optimisation process, a series of control reactions were undertaken. When the reaction was conducted in ambient light or in the dark no conversion of the starting materials was observed (Table 1, entries 10 and 11), highlighting that the process is initiated by LED light irradiation and ruling out a potential  $\text{S}_{\text{N}}2$  pathway between the *in situ* generated enolate and the difluoroalkyl halide **2a**. Further experiments supported the involvement of radical intermediates as the presence of TEMPO (3.0 equiv.) completely inhibited the formation of product **3a** with the TEMPO adduct of **2a** being formed instead (see ESI for further information†).

**Table 1** Initial result, select optimisation, and control experiments with catalyst **C1**



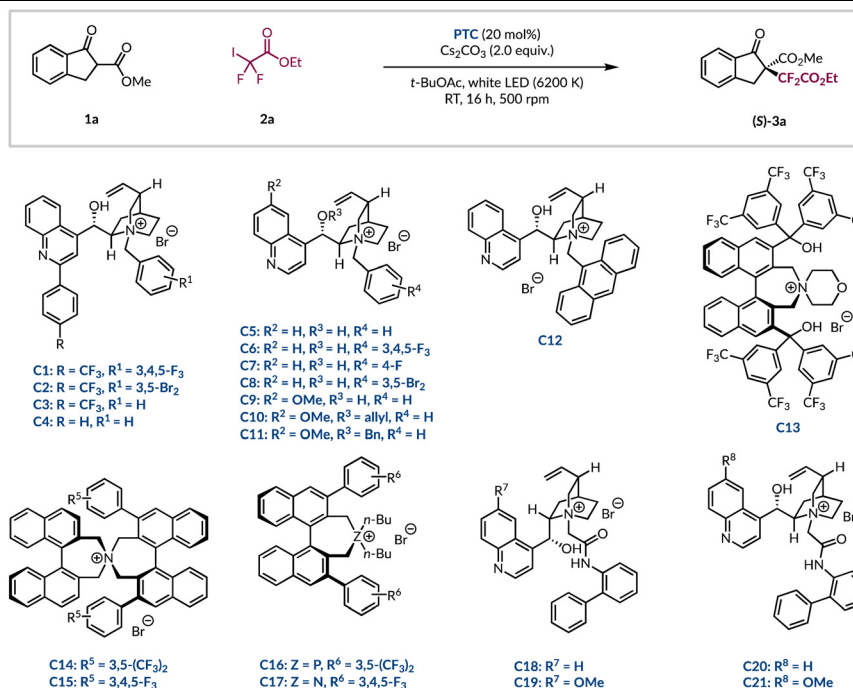
Entry	Deviation <sup>a</sup>	Solvent	<b>3a</b> <sup>b</sup> [%]	er <sup>c</sup>
1 <sup>d</sup>	—	PhCl: C <sub>8</sub> F <sub>18</sub> (2 : 1, 0.2 M)	10	57 : 43
2	—	CH <sub>2</sub> Cl <sub>2</sub> (0.1 M)	16	64 : 36
3	—	CHCl <sub>3</sub> (0.1 M)	95	68 : 32
4	—	<i>t</i> -BuOAc (0.1 M)	88	65 : 35
5	—	<i>t</i> -BuPh (0.1 M)	64	69 : 31
6	No <b>C1</b>	<i>t</i> -BuOAc (0.1 M)	52	N/A
7	No <b>C1</b>	<i>t</i> -BuPh (0.1 M)	76	N/A
8	K <sub>2</sub> CO <sub>3</sub> , instead of Cs <sub>2</sub> CO <sub>3</sub>	<i>t</i> -BuOAc (0.1 M)	81	52 : 48
9	CSOAc, instead of Cs <sub>2</sub> CO <sub>3</sub>	<i>t</i> -BuOAc (0.1 M)	70	62 : 48
10	Ambient light, instead of white LED	<i>t</i> -BuOAc (0.1 M)	0	N/A
11	Dark (vial wrapped in aluminium foil)	<i>t</i> -BuOAc (0.1 M)	0	N/A

<sup>a</sup> Unless otherwise stated optimization reactions run on a 0.10 mmol scale of **1a**, **2a** (2.0 equiv.), **C1** (20 mol%) and Cs<sub>2</sub>CO<sub>3</sub> (2.0 equiv.) in stated solvent for 16 h at RT, irradiated with white LED (6200 K). <sup>b</sup> Yield determined by <sup>1</sup>H NMR analysis of the crude reaction with 1,3,5-trimethoxybenzene (0.33 equiv.). <sup>c</sup> er [(S):(R)] determined by chiral HPLC. <sup>d</sup> Reaction performed for 64 h. See ESI for further details.†

### Phase-transfer catalyst evaluation

Subsequently, we investigated a range of alternative phase-transfer catalysts to determine if any would be able to outcompete the background reaction and improve the enantioselectivity of the difluoroalkylation process (Table 2). First, a series of 2-aryl quinoline substituted cinchonine catalysts (**C1–4**) were investigated. Replacing the 3,4,5-trifluorinated benzyl group with a 3,5-dibrominated analogue led to a noticeable drop in er (Table 2, entries 1 and 2).<sup>38,39</sup> Related catalysts (**C3–4**), which contain a simple benzyl group, showed that the *p*-CF<sub>3</sub> group on the other aryl ring was important as only racemic product (**3a**) was formed without it (Table 2, entries 3 and 4). Further investigations revealed that complete removal of the 2-aryl substituent on the quinoline core (**C5–C11**) was also detrimental as no enantioinduction was observed (Table 2, entries 5–11). Notably, this included catalyst **C6**, which has the same fluorinated benzyl group as **C1**. Even the introduction of the sterically cumbersome anthracenyl group in PTC **C12** did not restore the stereoselectivity (Table 2, entry 12). At this stage, it was decided to investigate phase-transfer catalysts with greater structural diversity. Having been implemented for the asymmetric functionalisation of  $\beta$ -ketoesters, as well as a vast range of other carbonyl-containing compounds, the Maruoka-type structures (**C13–17**) were considered to be ideal candidates to realise the desired transformation with high stereocontrol.<sup>15,16,40–43</sup> Unfortunately, from this selection of BINOL-derived catalysts no improvement



**Table 2** Screen of chiral phase-transfer catalysts for the enantioselective  $\alpha$ -difluoroalkylation of  $\beta$ -ketoester **1a**

Entry <sup>a</sup>	Catalyst	<b>3a</b> <sup>b</sup> [%]	er <sup>c</sup>
1	C1	88	65 : 35
2	C2	82	54 : 46
3	C3	69	63 : 37
4	C4	66	50 : 50
5	C5	75	50 : 50
6	C6	83	51 : 49
7	C7	79	51 : 49
8	C8	71	50 : 50
9	C9	67	51 : 49
10	C10	37	50 : 50
11	C11	55	50 : 50
12	C12	22	50 : 50
13	C13	73	50 : 50
14	C14	43	50 : 50
15	C15	72	50 : 50
16	C16	55	50 : 50
17	C17	61	50 : 50
18	C18	>99	26 : 74
19	C19	92	27 : 73
20	C20	78	68 : 32
21	C21	81	72 : 28

<sup>a</sup> Unless otherwise stated optimization reactions a 0.10 mmol scale of **1a**, **2a** (2.0 equiv.), PTC (20 mol%) and Cs<sub>2</sub>CO<sub>3</sub> (2.0 equiv.) in *t*-BuOAc (0.1 M) for 16 h at RT, irradiated with white LED 6200 K. <sup>b</sup> Yield determined by <sup>1</sup>H NMR analysis of the crude reaction with 1,3,5-trimethoxybenzene (0.33 equiv.). <sup>c</sup> er [(S) : (R)] determined by chiral HPLC.

over the *N*-benzylated cinchona alkaloid derivatives was found and only racemic **3a** was generated (Table 2, entries 13–17). In 2017, Li and co-workers performed a DFT study that highlighted the extent to which a core network of H-bonding interactions dictated the high levels of asymmetric induction in the analogous perfluoroalkylation reaction.<sup>44</sup> Inspired by this, it was decided to investigate more recently developed cinchona-based PTCs bearing arylated amides in lieu of benzyl groups from Jurczak.<sup>45</sup> These organocatalysts have enjoyed broad appli-

cations with a range of substrates, including with  $\beta$ -ketoesters.<sup>46–48</sup> The biphenyl amide was appended to the four common cinchona alkaloids to give catalysts **C18–21**. These all eclipsed PTC **C1** giving the highest yields of enantioenriched product **3a** seen thus far (Table 2, entries 1 vs. 18–21). In general, it was found that the amide motif, which provides additional hydrogen bonding capabilities, was superior to its direct benzylated analogues (*e.g.* **C20** vs. **C5–8**). The cinchonidine scaffold of PTC **C18** marginally outperformed the other



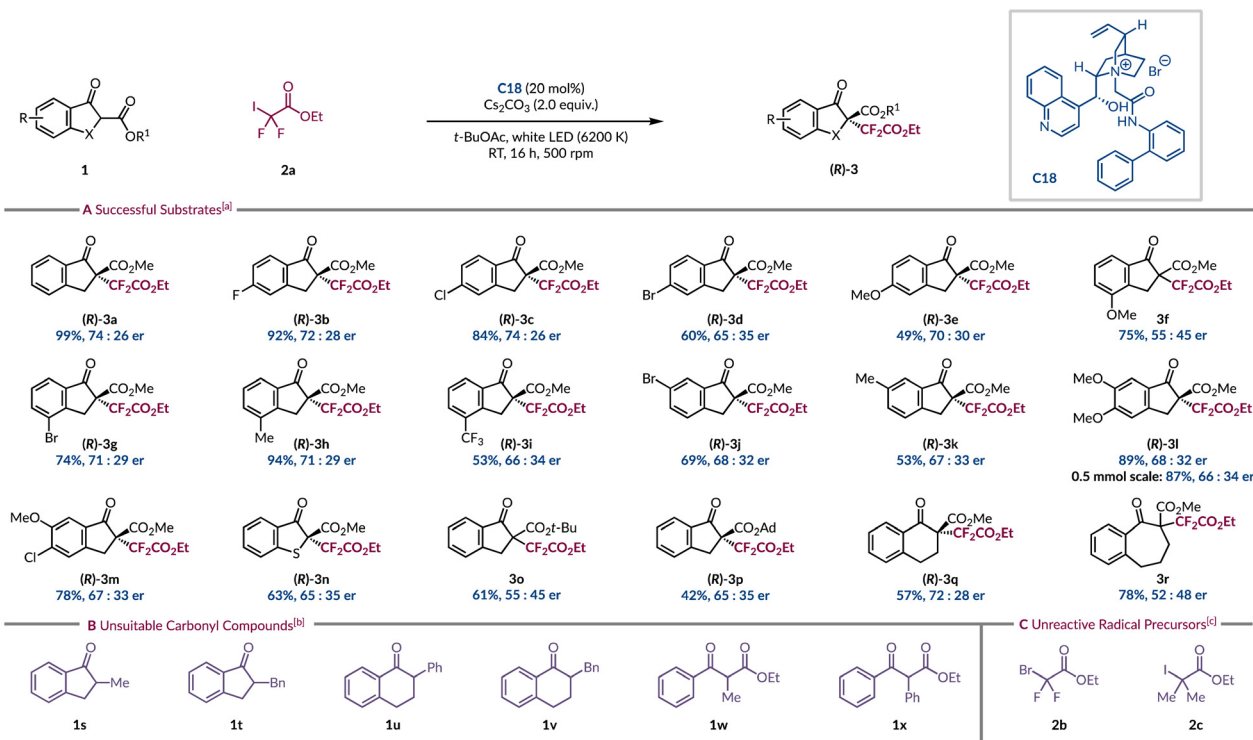
alkaloid architectures (**C19–21**) to give difluoroalkylated  $\beta$ -ketoester **3a** in quantitative yield and 76 : 24 er (Table 2, entry 18). Further optimisation of the reaction parameters with PTC **C18** was carried out, but any deviation from the standard conditions had a negative impact on both yield and stereocontrol (see ESI page S21†). As an exhaustive optimization process had been carried out, it was deemed appropriate to initiate an investigation into the scope of this methodology.

### Substrate scope

With the optimised conditions in hand, a variety of  $\beta$ -ketoesters with differing electronic and steric demands, as well as diverse aryl substitution patterns was explored (Scheme 1A). Interestingly, a clear trend did not emerge that would enable us to holistically rationalise how these changes impacted the yield and enantioselectivity of the reaction. Introducing a 5-fluoro substituent on the indanone ring had a minimal effect as the expected product **3b** was isolated in 92% yield with 72 : 28 er. A chlorine atom was equally tolerated at this position (**3c**), but the larger brominated analogue (**3d**) did suffer from a drop in yield and er. An electron-rich methoxy group in the same site (**3e**) led to a further decline in yield but with moderate levels of asymmetric induction. Relocating the OMe substituent to the 4-position provided product **3f** in good yield, although with 55 : 45 er. Replacing the 4-substituent

with either a bromine atom (**3g**) or a methyl group (**3h**) restored the standard level of enantioenrichment. The yield and enantioselectivity were negatively influenced by the presence of an electron-deficient 4-trifluoromethyl group (**3i**). The bromine atom was best tolerated at the 4-site (**3g**) as lower yields and enantiomeric ratios were obtained at either the 5- or 6-position (**3d** & **3j**). A similar slight detrimental effect was observed with the 6-methyl product **3k**. 5,6-Disubstituted  $\beta$ -ketoesters were also evaluated with 5,6-diMeO (**3l**) and 5-Cl-6-MeO (**3m**) both giving similar enantioselectivities to those observed for 6-monosubstituted analogues. For product **3l** comparable results were obtained on a 0.5 mmol scale. The introduction of a sulfur atom at the 3-position of the indanone motif afforded product **3n** in 63% yield with 65 : 35 er, which when compared to the sulfur-free analogue **3a** shows a lower asymmetric induction.

Previous studies have recognised that the steric bulk of the ester of  $\beta$ -ketoester **1a** can result in excellent levels of stereocontrol during product formation when intercepting fluorinated carbon-centred radicals.<sup>12,14</sup> To our surprise this strategy failed to yield the same benefit in our system as substrate **1o**, bearing a *t*-butyl ester, led to a near racemic product (**3o**). Given this was the standard substrate for Melchiorre and co-workers in their related work, it again highlights the huge impact the modification of the radical precursor has had on



**Scheme 1** (A) Substrate scope for the light-initiated phase-transfer-catalysed asymmetric  $\alpha$ -difluoroalkylation of  $\beta$ -ketoesters; (B) carbonyl compounds that were tested but unsuccessful; (C) alternative radical precursors that were unreactive. <sup>a</sup>Unless otherwise stated reactions were run on a 0.10 mmol scale of **1a**, **2a** (2.0 equiv.), **C18** (20 mol%) and  $\text{Cs}_2\text{CO}_3$  (2.0 equiv.) in *t*-BuOAc (0.1 M) for 16 h at RT, irradiated with white LED (6200 K), isolated yields are stated, er determined by chiral HPLC. Racemic reactions were run by replacing **C18** with  $\text{Bu}_4\text{NBr}$  (20 mol%) <sup>b</sup>Unsuccessful cyclic and acyclic carbonyl substrates under both racemic and asymmetric protocols (see ESI for full details†). <sup>c</sup>Radical precursors that were unreactive under both racemic and asymmetric protocols with a variety of carbonyl substrates (see ESI for full details†).



the overall efficiency of the process.<sup>14</sup> The larger 1-adamantyl ester (**3p**) was also tested, resulting in the lowest yield among the various esters. Although, the enantiocontrol was less affected compared to the *t*-butyl ester **3o**. Two distinct substrate binding modes have been proposed for cyclic  $\beta$ -ketoesters with amide-containing cinchona alkaloids. One involves a hydrogen bond between the catalyst and the carbonyl of the ester, while the other does not invoke such a non-covalent interaction.<sup>47,49</sup> Increasing the steric bulk of the ester may influence its ability to engage in hydrogen bonding with PTC **C18**. Product **3p** enabled the absolute configuration of the major enantiomer to be determined by comparing its specific rotation to a literature value,<sup>12</sup> and the remaining products have been assigned by analogy. Lastly, we explored modifying the ring size from indanone (**3a**) to tetralone (**3q**), which resulted in a lower yield, but with near identical stereoselectivity. Further ring expansion was not tolerated as 7-membered carbocyclic product **3r** was afforded as a near racemate. Having explored a range of cyclic  $\beta$ -ketoesters we were keen to evaluate a wider array of carbonyl compounds to establish the differences in their reactivity and selectivity (Scheme 1B). A series of benzannulated  $\alpha$ -alkyl and  $\alpha$ -aryl substituted cyclic ketones (**1s–v**) all displayed no reactivity with full recovery of the starting materials. We believe that the formation of the EDA complex was not occurring with these substrates due to their higher  $pK_a$  relative to  $\beta$ -ketoesters. To facilitate the formation of the required enolate we switched to a stronger inorganic base ( $\text{CsOH}\cdot\text{H}_2\text{O}$ ) but to no avail. We also tested acyclic  $\beta$ -ketoesters (**1w–x**), but the desired products were not observed, alluding to the high substrate specificity for reactivity under these conditions. Ultimately, we redirected our focus towards exploring different radical precursors to determine whether they exhibited comparable restrictions (Scheme 1C). We hoped that the brominated form (**2b**) of the ethyl halodifluoroacetate reagent would quell undesired background activity, which might improve the enantioenrichment of the products. Unfortunately, no reactivity was witnessed at all even with the addition of common photocatalysts (see ESI page S27†). We also found that replacing the *geminal* fluorine atoms of **2a** with methyl groups (**2c**) impeded the formation of the radical.

### Mechanistic investigations into radical generation and background reactivity

Intrigued by the high efficiency of the reaction in non-polar solvents with an inorganic base in the absence of a phase-transfer catalyst (Table 1, entries 6 and 7), we sought to gain further insight into these reactions. First, we used UV-vis spectroscopy to determine if the photoexcitation of an individual reaction component or an EDA complex was responsible for the generation of the ethyl difluoroacetate radical (Fig. 2). Catalyst **C1** was not used for these studies due to its evident absorption of visible light in solution. The spectra of both starting materials (**1a** and **2a**) alone, do not exhibit significant absorbance at the shortest wavelengths (>400 nm) emitted by the white LED used (Fig. 2, blue and orange line). However, it

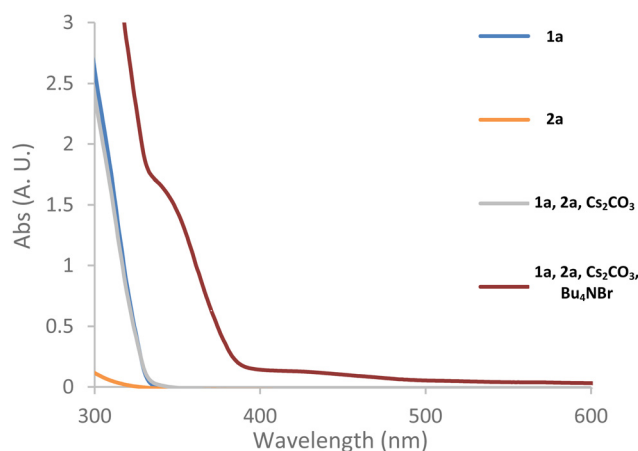
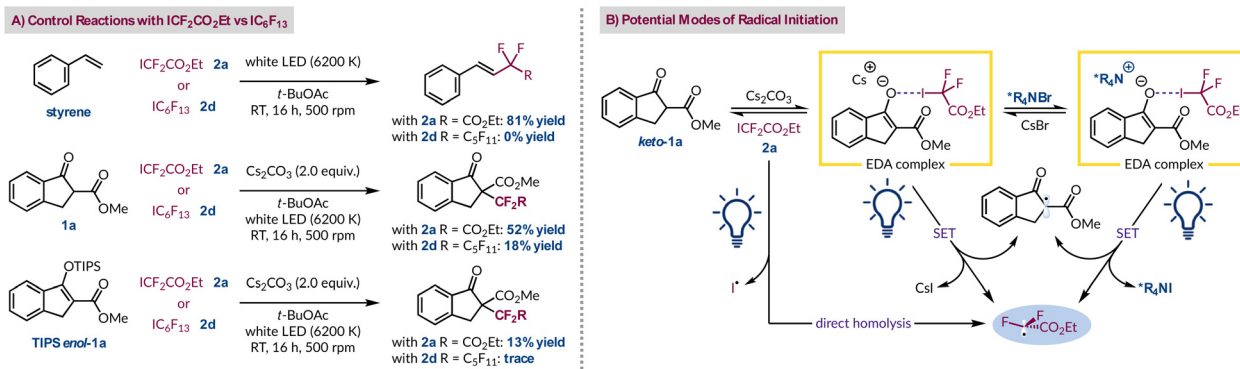


Fig. 2 UV-vis absorption spectra of the typical reaction mixture and its components in *t*-BuOAc. See ESI page S22 for full experimental details and more in-depth discussion.†

should be noted that commercial samples of ester **2a** tend to have a pink hue due to trace amounts of iodine. This has been identified as the reason for its apparent absorption of visible light as freshly purified material, as used for our UV-vis absorption studies, does not absorb appreciably in the visible region.<sup>30</sup> The combination of **1a** and **2a** with  $\text{Cs}_2\text{CO}_3$  in *t*-BuOAc did not generate any solution phase species with a different absorption profile from the starting materials (Fig. 2, grey line). However, the solid phase of the mixture was orange indicating the formation of an EDA complex on the surface of the inorganic base. The subsequent addition of the achiral phase-transfer catalyst, tetrabutylammonium bromide, led the previously colourless organic liquid layer to develop a yellow/orange hue – indicating the EDA complex had been successfully transported into the liquid phase. This was confirmed by UV-vis spectroscopy as a noticeable bathochromic shift towards the visible light region was observed (Fig. 2, red line). Therefore, in the presence of a phase-transfer catalyst, we believe that this EDA complex is contributing to the production of the ethyl difluoroacetate radical. However, the mode of radical initiation in the absence of a phase-transfer catalyst remained nebulous.

Therefore, to probe the radical formation step, and further our understanding of why the fluorinated radical precursors **2a** and **2d** give vastly different outcomes,<sup>14</sup> a series of control experiments were conducted (Fig. 3A). Using styrene as the radical acceptor in the absence of base gave the expected product with ester-containing **2a**, but not with perfluorohexyl iodide (**2d**).<sup>35,50</sup> Under these conditions there is no spectroscopic evidence to suggest an EDA complex is forming, indicating that the direct homolysis of **2a** occurs more readily than for **2d**.<sup>35</sup> This occurs despite poor spectral overlap between the emission spectrum of the white LED and the absorption spectrum of radical precursor **2a**. However, this corroborates our observation that purified and colourless **2a** turns pink in ambient light due to the liberation of iodine, but **2d** remains





**Fig. 3** (A) A series of reactions that evaluate the differences between ICF<sub>2</sub>CO<sub>2</sub>Et and IC<sub>6</sub>F<sub>13</sub> under identical reaction conditions (B) postulated pathways for the generation of the ethyl difluoroacetate radical in this system.

colourless. In the context of comparing their background reactivity both radical progenitors were tested with  $\beta$ -ketoester **1a** in the absence of a PTC. Both generated their respective products in 52% yield (**2a**) and 18% yield (**2d**), highlighting the greater extent of background reactivity with **2a**. Given that direct homolysis of **2d** was not previously witnessed implies that the cesium enolate of **1a** can promote radical formation by excitation of its EDA complex with **2d**. Using TIPS-protected **1a**, which is an inferior electron donor, demonstrated lower reactivity and only afforded traces of product with precursor **2d**. We rationalise that this is because the only route now available for radical initiation is direct homolysis of the C–I bond, which only occurs for **2a**. Consequently, we can deduce that three different processes can account for the formation of the ethyl difluoroacetate radical from **2a** under phase-transfer conditions (Fig. 3B). In the absence of the quaternary ammonium salt, two of these pathways remain available for reagent **2a**, but only one route, an EDA complex with the Cs enolate, is feasible for precursor **2d**.

Lastly, having considered the different pathways for the radical initiation step we also pondered the various mechanisms through which the new C–C bond could form (Fig. 4). Under asymmetric phase-transfer conditions the desired addition of the ethyl difluoroacetate radical to **\*R<sub>4</sub>N enolate-1a** must be occurring due to the non-racemic production of product **3a**. However, without the PTC the reaction still proceeds efficiently and must follow a distinct C–C bond forming event. One viable option is that the radical adds to **enol-1a**, which is observed by <sup>1</sup>H NMR spectroscopy to varying degrees for the different  $\beta$ -ketoester substrates. Considering TIPS **enol-1a** as a model for this tautomeric form we have shown that it is a viable radical acceptor (Fig. 3A). Similarly, the fact that Cs **enolate-1a** was implicated in the formation of an EDA complex with perfluorohexyl iodide (**2d**) indicates that it is also present in solution. Radical addition to this species would also lead to racemic product **3a**. A third possibility is radical–radical coupling between the  $\alpha$ -keto radical and ethyl difluoroacetate radical formed after photoexcitation of the EDA complex. However, this would be polarity mismatched as both radicals

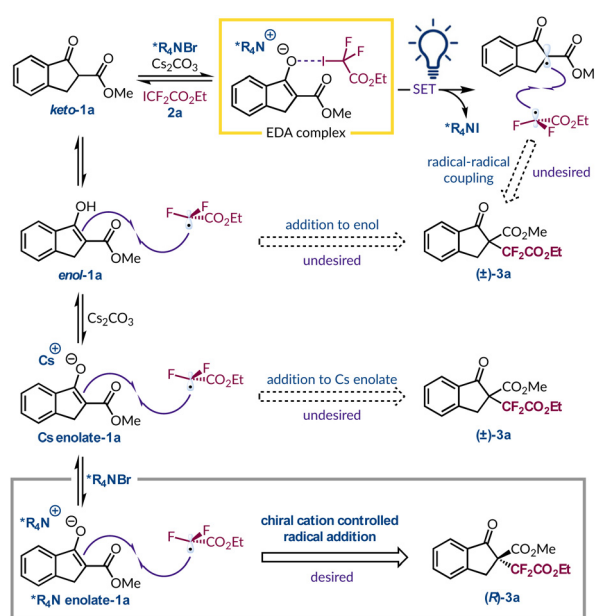


**Fig. 4** Outline of the different pathways for racemic and enantioselective product formation.

are generally considered to be electrophilic.<sup>51</sup> The heterogeneity of the reaction mixture thwarted attempts to determine the quantum yield under mechanistically relevant conditions, which would have helped clarify if radical–radical coupling or a chain process was dominant. Although, based on the philicity of the radicals involved and the fact that the fluorinated electrophilic radical is certainly adding to the electron-rich **\*R<sub>4</sub>N enolate-1a**, and this could conceivably lead to a chain process as outlined previously,<sup>14</sup> we do not think radical–radical coupling is operating appreciably under phase-transfer or PTC-free conditions. Thus, the more facile production of radicals from **2a** compared to **2d** is likely interacting with either the more abundant **enol-1a** or its more electron-rich deprotonated form (**Cs enolate-1a**). However, we cannot distinguish between these two pathways at present and our



attempts to slow radical formation, for example, by changing the irradiation wavelength, were not beneficial.

### 3. Conclusion

In conclusion, we have developed a light-initiated asymmetric tertiary  $\alpha$ -difluoroalkylation procedure that operates under mild phase-transfer conditions. Impressively, despite pronounced background reactivity moderate levels of asymmetric induction were still achievable. When using a PTC, UV-vis spectroscopic evidence suggests that a solution-phase visible light-absorbing EDA complex is responsible for radical initiation. However, contributions from other pathways, evident in the absence of a PTC, may also operate alongside to generate the ethyl difluoroacetate radical. We conducted several control experiments to determine why the behaviour of the two radical precursors (**2a** and **2d**) was so different, but we were unable to come to a definite conclusion. Further studies will seek to address these challenges and broaden the scope of asymmetric radical reactions carried out under phase-transfer conditions.

### Data availability

The research data underpinning this publication can be accessed at <https://doi.org/10.17630/301fa354-0637-4065-a526-fbc7c3a3f462>.

### Author contributions

C. E. A.: methodology, investigation, writing. C. P. J.: conceptualization, methodology, writing, supervision, project administration, funding acquisition.

### Conflicts of interest

There are no conflicts to declare.

### Acknowledgements

The authors acknowledge funding from the Royal Society (University Research Fellowship URF/R1\180017 (CPJ)) and the University of St Andrews (CEA). We thank Yitong Wang for his help in the synthesis of starting materials and Reece Hoogesteger for running scale-up experiments. We thank Prof. Andy Smith, Prof. Allan Watson, and their respective research groups for sharing their lab equipment and chemical inventories.

### References

- 1 T. Lasing, A. Phumee, P. Siriyasatien, K. Chitchak, P. Vanalabhpatana, K.-K. Mak, C. H. Ng, T. Vilaivan and T. Khotavivattana, Synthesis and antileishmanial activity of fluorinated rhodacyanine analogues: The 'fluorine-walk' analysis, *Bioorg. Med. Chem.*, 2020, **28**, 115187.
- 2 A. Vulpetti and C. Dalvit, Fluorine local environment: from screening to drug design, *Drug Discovery Today*, 2012, **17**, 890–897.
- 3 A. D. Dilman and V. V. Levin, Difluorocarbene as a Building Block for Consecutive Bond-Forming Reactions, *Acc. Chem. Res.*, 2018, **51**, 1272–1280.
- 4 K. Müller, C. Faeh and F. Diederich, Fluorine in Pharmaceuticals: Looking Beyond Intuition, *Science*, 2007, **317**, 1881–1886.
- 5 S. Purser, P. R. Moore, S. Swallow and V. Gouverneur, Fluorine in medicinal chemistry, *Chem. Soc. Rev.*, 2008, **37**, 320–330.
- 6 T. Liang, C. N. Neumann and T. Ritter, Introduction of Fluorine and Fluorine-Containing Functional Groups, *Angew. Chem., Int. Ed.*, 2013, **52**, 8214–8264.
- 7 M. Fornalczyk, K. Singh and A. M. Stuart, Enantioselective Reformatsky reaction of ethyl iododifluoroacetate with ketones, *Org. Biomol. Chem.*, 2012, **10**, 3332–3342.
- 8 P. Zhang and C. Wolf, Catalytic Enantioselective Difluoroalkylation of Aldehydes, *Angew. Chem., Int. Ed.*, 2013, **52**, 7869–7873.
- 9 X. Gao, Y.-L. Xiao, X. Wan and X. Zhang, Copper-Catalyzed Highly Stereoselective Trifluoromethylation and Difluoroalkylation of Secondary Propargyl Sulfonates, *Angew. Chem., Int. Ed.*, 2018, **57**, 3187–3191.
- 10 H. Liang, G.-Q. Xu, Z.-T. Feng, Z.-Y. Wang and P.-F. Xu, Dual Catalytic Switchable Divergent Synthesis: An Asymmetric Visible-Light Photocatalytic Approach to Fluorine-Containing  $\gamma$ -Keto Acid Frameworks, *J. Org. Chem.*, 2019, **84**, 60–72.
- 11 X. Gao, R. Cheng, Y.-L. Xiao, X.-L. Wan and X. Zhang, Copper-Catalyzed Highly Enantioselective Difluoroalkylation of Secondary Propargyl Sulfonates with Difluoroenoxy silanes, *Chem*, 2019, **5**, 2987–2999.
- 12 J. Liu, W. Ding, Q.-Q. Zhou, D. Liu, L.-Q. Lu and W.-J. Xiao, Enantioselective Di-/Perfluoroalkylation of  $\beta$ -Ketoesters Enabled by Cooperative Photoredox/Nickel Catalysis, *Org. Lett.*, 2018, **20**, 461–464.
- 13 S. Huang, F.-F. Tong, D.-C. Bai, G.-P. Zhang, Y.-J. Jiang, B. Zhang, X. Leng, Y.-L. Guo, X.-L. Wan, X. Zhang, C.-H. Ding and X.-L. Hou, Regio- and enantioselective umpolung gem-difluoroalkylation of hydrazones via palladium catalysis enabled by N-heterocyclic carbene ligand, *Nat. Commun.*, 2021, **12**, 6551.
- 14 Ł. Woźniak, J. J. Murphy and P. Melchiorre, Photo-organocatalytic Enantioselective Perfluoroalkylation of  $\beta$ -Ketoesters, *J. Am. Chem. Soc.*, 2015, **137**, 5678–5681.
- 15 T. Ooi and K. Maruoka, Recent Advances in Asymmetric Phase-Transfer Catalysis, *Angew. Chem., Int. Ed.*, 2007, **46**, 4222–4266.



- 16 S. Shirakawa and K. Maruoka, Recent Developments in Asymmetric Phase-Transfer Reactions, *Angew. Chem., Int. Ed.*, 2013, **52**, 4312–4348.
- 17 R. S. J. Proctor, A. C. Colgan and R. J. Phipps, Exploiting attractive non-covalent interactions for the enantioselective catalysis of reactions involving radical intermediates, *Nat. Chem.*, 2020, **12**, 990–1004.
- 18 T. E. Schirmer and B. König, Ion-Pairing Catalysis in Stereoselective, Light-Induced Transformations, *J. Am. Chem. Soc.*, 2022, **144**, 19207–19218.
- 19 S. Mondal, F. Dumur, D. Gimes, M. P. Sibi, M. P. Bertrand and M. Nechab, Enantioselective Radical Reactions Using Chiral Catalysts, *Chem. Rev.*, 2022, **122**, 5842–5976.
- 20 M. J. Genzink, J. B. Kidd, W. B. Swords and T. P. Yoon, Chiral Photocatalyst Structures in Asymmetric Photochemical Synthesis, *Chem. Rev.*, 2022, **122**, 1654–1716.
- 21 D. C. M. Albanese and M. Penso, New Trends in Asymmetric Phase Transfer Catalysis, *Eur. J. Org. Chem.*, 2023, e202300224.
- 22 R. S. Mulliken, Structures of Complexes Formed by Halogen Molecules with Aromatic and with Oxygenated Solvents<sup>1</sup>, *J. Am. Chem. Soc.*, 1950, **72**, 600–608.
- 23 R. S. Mulliken, Molecular Compounds and their Spectra. II, *J. Am. Chem. Soc.*, 1952, **74**, 811–824.
- 24 R. S. Mulliken, Molecular Compounds and their Spectra. III. The Interaction of Electron Donors and Acceptors, *J. Phys. Chem.*, 1952, **56**, 801–822.
- 25 R. Foster, Electron donor-acceptor complexes, *J. Phys. Chem.*, 1980, **84**, 2135–2141.
- 26 E. F. Hilinski, J. M. Masnovi, C. Amatore, J. K. Kochi and P. M. Rentzepis, Charge-transfer excitation of electron donor-acceptor complexes. Direct observation of ion pairs by time-resolved (picosecond) spectroscopy, *J. Am. Chem. Soc.*, 1983, **105**, 6167–6168.
- 27 S. V. Rosokha and J. K. Kochi, Fresh Look at Electron-Transfer Mechanisms via the Donor/Acceptor Bindings in the Critical Encounter Complex, *Acc. Chem. Res.*, 2008, **41**, 641–653.
- 28 G. E. M. Crisenza, D. Mazzearella and P. Melchiorre, Synthetic Methods Driven by the Photoactivity of Electron Donor–Acceptor Complexes, *J. Am. Chem. Soc.*, 2020, **142**, 5461–5476.
- 29 H.-R. Zhang, D.-Q. Chen, Y.-P. Han, Y.-F. Qiu, D.-P. Jin and X.-Y. Liu, Merging photoredox with copper catalysis: decarboxylative difluoroacetylation of  $\alpha,\beta$ -unsaturated carboxylic acids with ICF<sub>2</sub>CO<sub>2</sub>Et, *Chem. Commun.*, 2016, **52**, 11827–11830.
- 30 H. Lu, D. Wang and A. Zhang, Visible Light-Promoted Phosphine-Catalyzed Difluoroalkylation of Arenes and Heterocycles, *J. Org. Chem.*, 2020, **85**, 942–951.
- 31 X.-X. Liu, J. Jia, Z. Wang, Y.-T. Zhang, J. Chen, K. Yang, C.-Y. He and L. Zhao, Catalyst-Free and Visible Light Promoted Aminofluoroalkylation of Unactivated Alkenes: An Access to Fluorinated Aziridines, *Adv. Synth. Catal.*, 2020, **362**, 2604–2608.
- 32 T. Mao, M.-J. Ma, L. Zhao, D.-P. Xue, Y. Yu, J. Gu and C.-Y. He, A general and green fluoroalkylation reaction promoted via noncovalent interactions between acetone and fluoroalkyl iodides, *Chem. Commun.*, 2020, **56**, 1815–1818.
- 33 Y. Li, M. Rao, Z. Fan, B. Nian, Y. Yuan and J. Cheng, A visible-light-irradiated electron donor-acceptor complex-promoted radical reaction system for the CH perfluoroalkylation of quinolin-4-ols, *Tetrahedron Lett.*, 2019, **60**, 151046.
- 34 A. Lemos, C. Lemaire and A. Luxen, Progress in Difluoroalkylation of Organic Substrates by Visible Light Photoredox Catalysis, *Adv. Synth. Catal.*, 2019, **361**, 1500–1537.
- 35 K. Li, X. Zhang, J. Chen, Y. Gao, C. Yang, K. Zhang, Y. Zhou and B. Fan, Blue Light Induced Difluoroalkylation of Alkynes and Alkenes, *Org. Lett.*, 2019, **21**, 9914–9918.
- 36 L. Li, Y.-N. Ma, M. Tang, J. Guo, Z. Yang, Y. Yan, X. Ma and L. Tang, Photoredox-Catalyzed Oxydifluoroalkylation of Styrenes for Access to Difluorinated Ketones with DMSO as an Oxidant, *Adv. Synth. Catal.*, 2019, **361**, 3723–3728.
- 37 W.-W. Xu, L. Wang, T. Mao, J. Gu, X.-F. Li and C.-Y. He, Visible-light Promoted Atom Transfer Radical Addition–Elimination (ATRE) Reaction for the Synthesis of Fluoroalkylated Alkenes Using DMA as Electron-donor, *Molecules*, 2020, **25**, 508.
- 38 Y. Wang, Z. Zheng, M. Lian, H. Yin, J. Zhao, Q. Meng and Z. Gao, Photo-organocatalytic enantioselective  $\alpha$ -hydroxylation of  $\beta$ -keto esters and  $\beta$ -keto amides with oxygen under phase transfer catalysis, *Green Chem.*, 2016, **18**, 5493–5499.
- 39 Y. Wang, S. Wang, P. Qiu, L. Fang, K. Wang, Y. Zhang, C. Zhang and T. Zhao, Asymmetric  $\alpha$ -electrophilic difluoromethylation of  $\beta$ -keto esters by phase transfer catalysis, *Org. Biomol. Chem.*, 2021, **19**, 4788–4795.
- 40 T. Hashimoto and K. Maruoka, Recent Development and Application of Chiral Phase-Transfer Catalysts, *Chem. Rev.*, 2007, **107**, 5656–5682.
- 41 M. Kitamura, S. Shirakawa and K. Maruoka, Powerful Chiral Phase-Transfer Catalysts for the Asymmetric Synthesis of  $\alpha$ -Alkyl- and  $\alpha,\alpha$ -Dialkyl- $\alpha$ -amino Acids, *Angew. Chem., Int. Ed.*, 2005, **44**, 1549–1551.
- 42 X. Wang, Q. Lan, S. Shirakawa and K. Maruoka, Chiral bifunctional phase transfer catalysts for asymmetric fluorination of  $\beta$ -keto esters, *Chem. Commun.*, 2009, **46**, 321–323.
- 43 T. Ooi, Y. Arimura, Y. Hiraiwa, L. M. Yuan, T. Kano, T. Inoue, J. Matsumoto and K. Maruoka, Highly enantioselective monoalkylation of p-chlorobenzaldehyde imine of glycine tert-butyl ester under mild phase-transfer conditions, *Tetrahedron: Asymmetry*, 2006, **17**, 603–606.
- 44 C. Yang, W. Zhang, Y.-H. Li, X.-S. Xue, X. Li and J.-P. Cheng, Origin of Stereoselectivity of the Photoinduced Asymmetric Phase-Transfer-Catalyzed Perfluoroalkylation of  $\beta$ -Ketoesters, *J. Org. Chem.*, 2017, **82**, 9321–9327.
- 45 M. Majdecki, P. Niedbala and J. Jurczak, Amide-Based Cinchona Alkaloids as Phase-Transfer Catalysts: Synthesis and Potential Application, *Org. Lett.*, 2019, **21**, 8085–8090.



- 46 M. Majdecki, A. Tyszka-Gumkowska and J. Jurczak, Highly Enantioselective Epoxidation of  $\alpha,\beta$ -Unsaturated Ketones Using Amide-Based Cinchona Alkaloids as Hybrid Phase-Transfer Catalysts, *Org. Lett.*, 2020, **22**, 8687–8691.
- 47 P. Niedbała, M. Majdecki, P. Grodek and J. Jurczak, H-Bond Mediated Phase-Transfer Catalysis: Enantioselective Generating of Quaternary Stereogenic Centers in  $\beta$ -Keto Esters, *Molecules*, 2022, **27**, 2508.
- 48 Y. Wang, S. Wang, Y. Wu, T. Zhao, J. Liu, J. Zheng, L. Wang, J. Lv and T. Zhang, Fast, highly enantioselective, and sustainable fluorination of 4-substituted pyrazolones catalyzed by amide-based phase-transfer catalysts, *Org. Chem. Front.*, 2023, **10**, 2226–2233.
- 49 M. Majdecki, P. Grodek and J. Jurczak, Stereoselective  $\alpha$ -Chlorination of  $\beta$ -Keto Esters in the Presence of Hybrid Amide-Based Cinchona Alkaloids as Catalysts, *J. Org. Chem.*, 2021, **86**, 995–1001.
- 50 N. J. W. Straathof, S. E. Cramer, V. Hessel and T. Noël, Practical Photocatalytic Trifluoromethylation and Hydrotrifluoromethylation of Styrenes in Batch and Flow, *Angew. Chem., Int. Ed.*, 2016, **55**, 15549–15553.
- 51 F. Parsaee, M. C. Senarathna, P. B. Kannangara, S. N. Alexander, P. D. E. Arche and E. R. Welin, Radical philicity and its role in selective organic transformations, *Nat. Rev. Chem.*, 2021, **5**, 486–499.

